ORIGINAL RESEARCH

Iron Overload-Induced Osteocyte Apoptosis Stimulates Osteoclast Differentiation Through Increasing Osteocytic RANKL Production In Vitro

Jiancheng Yang[1,2] · Dandan Dong[2] · Xinle Luo[1,4] · Jianhua Zhou[1] · Peng Shang[2,3] · Hao Zhang[1,4]

Abstract

Iron overload is closely associated with osteoporosis, the potential cellular mechanism involved in decreased osteoblast differentiation and increased osteoclast formation. However, the effect of iron overload on the biological behavior in osteocytes has not been reported. This study aims to investigate the changes of osteocytic activity, apoptosis, and its regulation on osteoclastogenesis in response to iron overload. MLO-Y4 osteocyte-like cells and primary osteocytes from mice were processed with ferric ammonium citrate (FAC) and deferoxamine (DFO), the conditioned medium (CM) was harvested and co-cultured with Raw264.7 cells and bone marrow-derived macrophages (BMDMs) to induce them to differentiate into osteoclasts. Osteocyte apoptosis, osteoclast differentiation, osteocytic gene expression and protein secretion of receptor activator of nuclear factor κB ligand (RANKL) and osteoprotegerin (OPG) was examined. Excessive iron has a toxic effect on MLO-Y4 osteocyte-like cells. Increased cell apoptosis in MLO-Y4 cells and primary osteocytes was induced by iron overload. The osteoclastic formation, differentiation-related gene expression, and osteoclastic bone-resorption capability were significantly increased after treated with the CM from iron overload-exposed osteocytes. Excessive iron exposure significantly promoted the gene expression and protein secretion of the RANKL in MLO-Y4 cells. Addition of RANKL-blocking antibody completely abolished the increase of osteoclast formation and bone resorption capacity induced by the CM from osteocytes exposed to excessive iron. Moreover, the pan-caspase apoptosis inhibitor, QVD (quinolyl-valyl-O-methylaspartyl-[-2,6-difluorophenoxy]-methylketone) was used to inhibit osteocyte apoptosis. The results showed osteocyte apoptosis induced by iron overload was reduced by QVD and accompanied by the decrease of soluble RANKL (sRANKL) in supernatant. The increase of osteoclast formation and bone resorption capacity induced by the CM from osteocytes exposed to excessive iron was significantly decreased by QVD. These results indicated that iron overload-induced osteocyte apoptosis is required to regulate osteoclast differentiation by increasing osteocytic RANKL production. This study, for the first time, reveals the indirect effect of iron overload on osteoclast differentiation through regulating osteocytes.

Keywords Iron overload · Osteocytes · Cell apoptosis · Osteoclastogenesis · Bone resorption · Osteoporosis

✉ Peng Shang
  shangpeng@nwpu.edu.cn

✉ Hao Zhang
  zhanghaodoctor@hotmail.com

[1] Department of Spine Surgery, People's Hospital of Longhua, Affiliated Hospital of Southern Medical University, No. 38, Jinglong Construction Road, Shenzhen 518109, Guangdong, China

[2] Key Laboratory for Space Bioscience and Biotechnology, School of Life Sciences, Northwestern Polytechnical

University, 127 West Youyi Road, Beilin District, Xi'an 710072, Shaanxi, China

[3] Research & Development Institute of Northwestern Polytechnical University in Shenzhen, Shenzhen, China

[4] The Third School of Clinical Medicine, Southern Medical University, Shenzhen, China

 Springer

Introduction

Although iron is an essential element for all living organisms, excessive iron (iron overload) has detrimental effects on tissues and organs. Numerous case reports and clinical studies have demonstrated a close relationship in iron overload and osteoporosis [1]. Iron overload in animal model also shows serious bone loss, manifests as dramatically damaged bone microstructure [2]. In vitro, there is increasing evidence that excessive iron inhibits osteoblastic differentiation and bone formation [3], while promotes osteoclastic formation and bone resorption [4, 5]. In contrast, iron chelation can increase the biological activity of osteoblasts and restrain osteoclastic differentiation [6, 7]. As the largest number of cells in bone tissue, osteocytes compose 90% to 95% of all bone cells. However, there are no reports on how iron overload affects the function of osteocytes.

Osteocyte lie embedded within the mineralized matrix and act as an orchestrator of bone remodeling through coordinate of both osteoclast and osteoblast activity on bone surfaces [8]. Osteocyte can produce pro- and anti-osteoclastogenic cytokines, including receptor activator of NF-κB ligand (RANKL) and osteoprotegerin (OPG), which regulate bone resorption [9]. In particular, a progressive increase in bone mass because of a reduced number of osteoclasts which can be observed in mice lacking the RANKL specifically in osteocytes, indicating that osteocytes are the major source of RANKL in bone remodeling [10]. Earlier work demonstrated that apoptosis of osteocytes precedes temporally and spatially osteoclast-mediated resorption [11]. Subsequent studies showed that the apoptotic osteocytes trigger viable, neighbor osteocytes to increase expression of RANKL at microdamage sites in bone, thus activating bone resorption [12, 13]. Recent studies indicated osteocyte apoptosis plays a controlling and central role in stimulating osteocyte RANKL production and the activation of bone resorption leading to bone loss in disused mice [14]. These results reveal that osteocyte apoptosis leads to increased RANKL production in osteocytes, which in turn stimulates the activity of osteoclasts.

Osteocytes are descended from mesenchymal stem cells through osteoblast differentiation. There are already proofs that iron overload can induce apoptosis of mesenchymal stem cells and osteoblasts [15, 16]. Therefore, we hypothesize that iron overload can induce apoptosis of osteocytes and cause increased RANKL production, which ultimately leads to increased osteoclastogenesis and bone resorption. The present study was addressed to investigate osteocyte apoptosis induced by iron overload, and evaluate osteoclast differentiation in conditioned media (CM) from iron-exposed osteocytes.

Materials and Methods

Cell Culture

MLO-Y4 osteocyte-like cells was used in this study and kindly provided by Dr. Jean X. Jiang (University of Texas Health Science Center, San Antonio, TX, USA). MLO-Y4 cells were cultured in collagen-coated petri dish in alpha-MEM medium (α-MEM; Gibco, Grand Island, NY, USA) supplemented with 5% FBS (Gibco), 5% calf serum (Gibco), 2 mM L-glutamine, and 1% penicillin–streptomycin. RAW264.7 cells, an established macrophage cell line used for inducing osteoclast formation in the presence of RANKL (Pepro Tech, Rocky Hill, NJ, USA), purchased from the Cell Bank of Chinese Academy of Sciences (CAS; Shanghai, China). RAW264.7 cells were maintained in α-MEM supplemented with 10% FBS (Gibco), 2 mM L-glutamine, and 1% penicillin–streptomycin. The cells were cultured in 37 °C incubator with humidified 5% CO_2 atmosphere.

Isolation of Primary Bone Marrow Macrophages and Osteocytes

The femurs and tibias were aseptically removed from adult C57BL/6 mice and dissected free of adhering tissues. The bone ends were cut off with scissors and the marrow cavity was flushed with 0.01 M phosphate buffer solution (1 × PBS) by slowly injecting at one end of the bone using a sterile needle. The bone marrow cells were collected, washed with a-MEM, and removed red blood cells by treatment with red blood cell lysis buffer (Solarbio, Beijing, China). The cells were maintained in α-MEM supplemented with 10% FBS (Gibco), 2 mM L-glutamine, and 1% penicillin–streptomycin. Cells were cultured overnight and then the non-adherent cells were collected and treated with 20 ng/ml macrophage colony-stimulating factor (M-CSF; Pepro Tech) for 5 days to induce macrophages formation. Then, the induced bone marrow-derived macrophages (BMDMs) were seeded, and incubated with M-CSF (20 ng/ml) and RANKL (50 ng/ml) for differentiation into osteoclasts.

Osteocytes were isolated from the above bone which the marrow cavity has been flushed according to a protocol of Bonewald and co-workers [17]. Serial digestions with collagenase I (Gibco) and Ethylenediaminetetraacetic acid (EDTA) solution (Kemiou, Tianjin, China) were done alternately. The cells from digest fraction 8–9 were considered to be osteocytes. Moreover, after last digestion seeded the bone particles in petri dish. At next day the bone particles were transferred to a collagen-coated petri dish. Very important did not disturb the plates until day 5. Then, bone particles were discarded and adherent cells were identified as

osteocytes. Isolated primary osteocytes were cultivated in the same culture conditions as MLO-Y4 cells.

Cell Viability Assay

Cell viability assay was processed with the Cell Counting Kit 8 kit (Beyotime Biotechnology, Shanghai, China) according to the manufacturer's protocols. MLO-Y4 cells were seeded in 96-well cell culture plates and allowed to attach after 8 h. Cells were treated with different concentrations of ferric ammonium citrate (FAC; Sigma-Aldrich, St. Louis, MO, USA) or deferoxamine (DFO; Sigma-Aldrich) for 24 h. Then, 10% CCK-8 solution was added and incubated at 37 °C for 2 h. Optical density (OD) value was determined using a Synergy HT multimode microplate reader (BioTek, Winooski, Vermont, USA) at 450 nm.

Cell Apoptosis Assay

After the MLO-Y4 cells were cultured in serum-supplemented α-MEM, α-MEM with 20 μM DFO, α-MEM with 40 μM Fe (from FAC with 17% Fe), and α-MEM with 40 μM Fe and 20 μM DFO for 24 h, cells were stained using the Annexin V-FITC Apoptosis Detection Kit (Beyotime) following the manufacturer's instructions. Then, flow cytometry was performed by flow cytometric analysis (BD, Franklin Lakes, NJ, USA). The Annexin V^+/PI^- osteocytes were considered early apoptotic cells. The Annexin V^+/PI^+ osteocytes were considered late apoptotic cells.

To further confirm the level of osteocyte apoptosis, DNA fragmentation in MLO-Y4 cells and primary osteocytes was identified using the One Step TUNEL Apoptosis Assay Kit (Beyotime). Then, cells were immediately observed and photographed using a Nikon Eclipse 80i fluorescence microscope (Nikon, Tokyo, Japan). TUNEL-positive cells were marked with green fluorescence.

Conditioned Medium Collection

After the MLO-Y4 cells were cultured in serum-supplemented α-MEM, α-MEM with 20 μM DFO, α-MEM with 40 μM Fe (from FAC with 17% Fe), and α-MEM with 40 μM Fe and 20 μM DFO for 24 h, cells were washed twice with $1 \times PBS$ and subsequently cultured in serum-supplemented normal medium, and conditioned medium (CM) was harvested after 24 h. The collected CM was never frozen or allowed to age in any way.

Osteoclast Formation Assay

To induce osteoclast formation, Raw 264.7 cells were cultured in serum-supplemented α-MEM with 50 ng/ml soluble RANKL in terms of previous report [18]. After 24 h,

the medium was replaced with a mixture of 50% CM and 50% growth medium. This procedure was repeated every other day until day 4, the cells were washed and fixed in 4% formaldehyde solution for 20 min. Then, the cells were stained using a Leukocyte Acid Phosphatase kit (Sigma-Aldrich) according to the manufacturer's protocol. Cells were photographed using a light microscopy (Nikon) and were recognized as osteoclasts if they were tartrate-resistant acid phosphate (TRAP) positive and exhibited three or more nuclei. The number of formed osteoclasts was calculated by ImageJ software.

TRAP Activity Assay

TRAP activity in differentiated osteoclasts exposed to the mixed medium of CM and growth medium for 2 and 4 days (d) was examined by TRAP assay kit (Beyotime). TRAP activity was evaluated based on the conversion of para-nitrophenyl phosphate (c) to para-nitrophenol (pNP) in the presence of tartrate solution. OD value was detected at 405 nm using a microplate reader (BioTek, Winooski, Vermont, USA), calculating the generated pNP levels according to the standard curve. The amount of acid phosphatase required to hydrolyze the pNPP chromogenic substrate per minute to produce 1 μM pNP was taken as one enzyme activity unit (U), and the TRAP activity is expressed as the enzyme activity per μg protein. The content of total protein in osteoclasts was determined using the BCA Protein Assay Kit (Beyotime).

Osteoclastic Bone Resorption Capability

RAW264.7 cells were seeded in the Osteo Assay Surface 96-well plates (Corning, NY, USA) at the density of 5,000 cells/well. The same differentiation procedure as the osteoclast formation assay was performed and repeated every other day until day 10. The medium was removed and 10% sodium hypochlorite was added to the wells and incubated at room temperature for 10 min. Subsequently, the wells were washed with deionized water and dried. Images in the bottom of wells were required using a light microscopy (Nikon). Osteoclastic bone resorption capability was evaluated by ImageJ software and expressed as the ratio of the pits area to the total area of the photograph.

F-actin Staining

After Raw264.7 cells were induced to differentiate into osteoclasts in the mixed medium of CM and growth medium for 4 d, the cells were stained using rhodamine-labeled phalloidin (Invitrogen, Carlsbad, CA, USA) overnight. Next, the cells were washed with $1 \times PBS$ three times and dried. The f-actin filaments were observed and photographed using a

fluorescence microscope (Nikon). The number of formed actin rings was calculated by ImageJ software.

Detection of Soluble Cytokines Secreted by Osteocytes

The concentration of soluble cytokines secreted by osteocytes in the collected CM, including soluble OPG and RANKL, was examined using the Mouse Osteoprotegerin/TNFRSF11B Quantikine enzyme linked immunosorbent assay (ELISA) Kit and the Mouse TRANCE/RANK L/TNFSF11 Quantikine ELISA Kit (R&D, Minneapolis, MN, China) according to the instructions of manufacturer, respectively.

Quantitative Real-Time PCR

After the CM was collected, total RNA in osteocytes was extracted using a HiPure Total RNA Mini Kit (Magen, Guangzhou, China). RNA was performed to reverse transcription using the HiScript II Q RT SuperMix (Vazyme, Nanjing, China) according to the manufacturer's instructions. Primers were sought in the Primer Bank and synthesized in Sangon Biotech (Shanghai, China), 1 μg cDNA as a template, were then used for quantitative real-time PCR with chamQ SYBR qPCR Master Mix (Vazyme) using CFX96 Touch qPCR System (Bio-Rad Laboratories, Hercules, CA, USA). The expression of the target genes was normalized to the respective GAPDH level. The sequences of primers are shown in Table 1.

RANKL Blocking

Neutralizing antibody (AB) specific for RANKL (Affinity, Cincinnati, OH, USA) were used to block specific proteins in the CM. AB of 1 μg/ml were incubated with CM at 37 ℃ for 1 h prior to adding to cells. Osteoclast formation, bone resorption, and f-actin staining experiments were subsequently performed as above.

Apoptosis Inhibition

QVD (MCE, Monmouth Junction, NJ, USA), the pan-caspase apoptosis inhibitor, has been used in previous study to prevent osteocyte apoptosis in vivo or in vitro [14]. MLO-Y4 cells and primary osteocytes were treated with QVD at 5 μM to inhibit cell apoptosis induced by iron overload.

Statistical Analysis

All experiments were performed in duplicate. More than three samples were examined in each assay. All data were presented as mean ± standard deviation (SD). The Student *t*

Table 1 Sequence of primers used for quantitative real-time PCR

Genes	Primers	Primer sequence (5′–3′)
BAX	Forward	ATGGGCTGGACACTGGACTTC
	Reverse	TCTTCCAGATGGTGAGCGAGG
BCL-2	Forward	TGTGTGGAGAGCGTCAACAG
	Reverse	CATCCCAGCCTCCGTTATCC
NFATc1	Forward	CCAGCTTTCCAGTCCCTTCC
	Reverse	ACTGTAGTGTTCTTCCTCGGC
MMP9	Forward	CTGGACAGCCAGACACTAAAG
	Reverse	CTCGCGGCAAGTCTTCAGAG
integrin β3	Forward	CCACACGAGGCGTGAACTC
	Reverse	CTTCAGGTTACATCGGGGTGA
CTSK	Forward	GAAGAAGACTCACCAGAAGCAG
	Reverse	TCCAGGTTATGGGCAGAGATT
RANKL	Forward	CAGCATCGCTCTGTTCCTGTA
	Reverse	CTGCGTTTTCATGGAGTCTCA
OPG	Forward	TACCTGGAGATCGAATTCTGCTT
	Reverse	CCATCTGGACATTTTTTGCAA

test was used to compare the difference between the Fe-CM group and the Fe-CM + RANKL AB group, and the Fe-CM group and the Fe + QVD-CM group. The other data were analyzed based on one-way ANOVA with Dunnett's multiple comparisons test. Differences were considered to be significant at $p < 0.05$. All statistical analysis was performed using the GraphPad Prism 7.0 software (La Jolla, CA, USA).

Results

Effects of Iron on Cell Viability in MLO-Y4 Cells

In present study, the CCK-8 assay results indicated that iron had toxic effects. After a 24 h exposure to FAC, the viability of MLO-Y4 cells was found to be significantly inhibited by iron exceeding 20 μM in a dose-dependent manner (Fig. 1a). Furthermore, the iron chelator DFO over 20 μM also decreased the viability of MLO-Y4 cells in a dose-dependent manner (Fig. 1b).

Iron Overload Induces Osteocyte Apoptosis

As shown in Fig. 2a and b, TUNEL staining for DNA fragmentation showed that cell apoptosis in MLO-Y4 cells and primary osteocytes can be elevated by excessive iron. The quantitative analysis of apoptosis by flow cytometry also revealed that Fe exposure with 40 μM significantly increased the cell apoptosis in MLO-Y4 cells (Fig. 2c and d). In contrast, iron overload-induced enhancement effect on osteocyte apoptosis was eliminated by DFO of 20 μM. Furthermore, iron overload exposure markedly upregulated proapoptotic
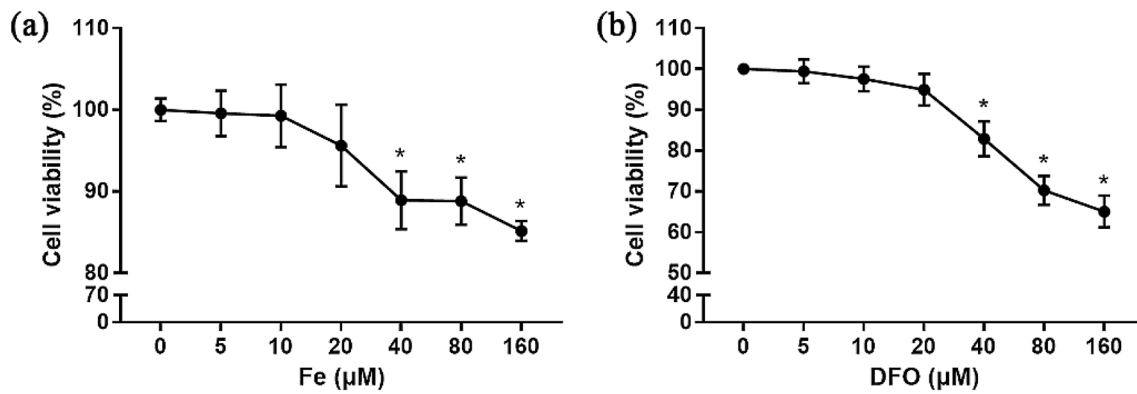
Fig. 1 Cytotoxic effects of iron on the viability of osteocytes. Viability of osteocytes was evaluated by CCK-8 assay after treatment with Fe (from FAC) (**a**) and DFO (**b**) for 24 h. Data are presented as the mean $\pm$ standard deviation ($n = 5$). $*P < 0.05$ compared with 0 μM

BAX gene expression while downregulated antiapoptotic BCL-2 expression, thus the BAX/BCL-2 ratio was dramatically enhanced by excessive iron in osteocytes after excessive iron loading (Fig. 2e).

Osteoclast Differentiation is Promoted by the CM from Fe-exposed Osteocytes

TRAP is highly expressed in osteoclasts, thus osteoclast formation is generally evaluated by TRAP staining. Compared with the Ctrl-CM group, the number of TRAP-positive multinucleated cells was increased in the CM from Fe-treated osteocytes (Fig. 3a). Furthermore, the CM from Fe-processed osteocytes significantly promoted TRAP activity at 2 and 4 d of osteoclast differentiation (Fig. 3b). In gene levels, the expression of some genes related to osteoclastogenesis, including NFATc1, MMP9, Integrin β3, and CTSK, was markedly higher the Fe-CM group than the Ctrl-CM group (Fig. 3c). The CM from DFO and Fe + DFO exposed osteocytes had no any effects on osteoclast differentiation.

Bone Resorption Capacity of Osteoclast is Enhanced by the CM from Fe-exposed Osteocytes

Osteoclasts can degrade bone matrix by secreting some proteases, a process known as bone resorption. Herein, osteoclastic bone resorption ability was examined by pit formation assay. The area of pits in the Fe-CM group was higher than the Ctrl-CM group (Fig. 4a). Mature osteoclasts can form a circle of actin (actin rings) which fix themselves to the bone surface and constitute a closed area to degrade bone matrix. In consequence, the formation of actin rings can be used as a marker to evaluate the bone resorption capacity of osteoclast. Compared with the Ctrl-CM group, the CM from Fe-processed osteocytes significantly elevated the number of actin rings on day 4 of osteoclast differentiation (Fig. 4b). There were no any effects of the CM from

DFO and Fe + DFO treated osteocytes on osteoclastic bone resorption capacity.

Effects of Iron Overload on RANKL/OPG Gene Expression and Secretion in MLO-Y4 Cells

We examined gene levels of RANKL and OPG in osteocytes to evaluate if apoptosis affected the expression of RANKL and OPG in osteocytes. Iron overload loading on MLO-Y4 cells increased the expression of RANKL gene. Although the gene level of OPG was not altered, the increase in RANKL contributed to a significant increase in RANKL/OPG ratio under excessive iron exposure (Fig. 5a). Considering our observed changes in RANKL gene expression, we next investigated whether iron overload may cause MLO-Y4 cells to produce a higher amount of soluble RANKL (sRANKL). We collected CM from iron-exposed osteocytes and measured the amount of sRANKL and soluble OPG (sOPG) using ELISA. The results showed excessive iron exposure remarkably increased the concentration of sRANKL in the CM from Fe-treated osteocytes, whereas iron overload stimulation did not alter the levels of sOPG (Fig. 5b). The sRANKL/sOPG ratio in the CM from Fe-processed osteocytes was also observably higher than that in the Control group. Furthermore, when the excess iron in osteocytes was chelated by DFO, the increased RANKL secretion and gene expression returned to the control levels.

Blocking RANKL in the CM from Fe-exposed Osteocytes Inhibits Osteoclastic Formation and Bone Resorption Capacity

To confirm if the apoptosis-induced increase in osteoclast differentiation are indeed due to the increased RANKL protein secretion, we applied a RANKL-blocking antibody to the CM from iron-exposed osteocytes prior to incubating with Raw264.7 cells. The results demonstrated
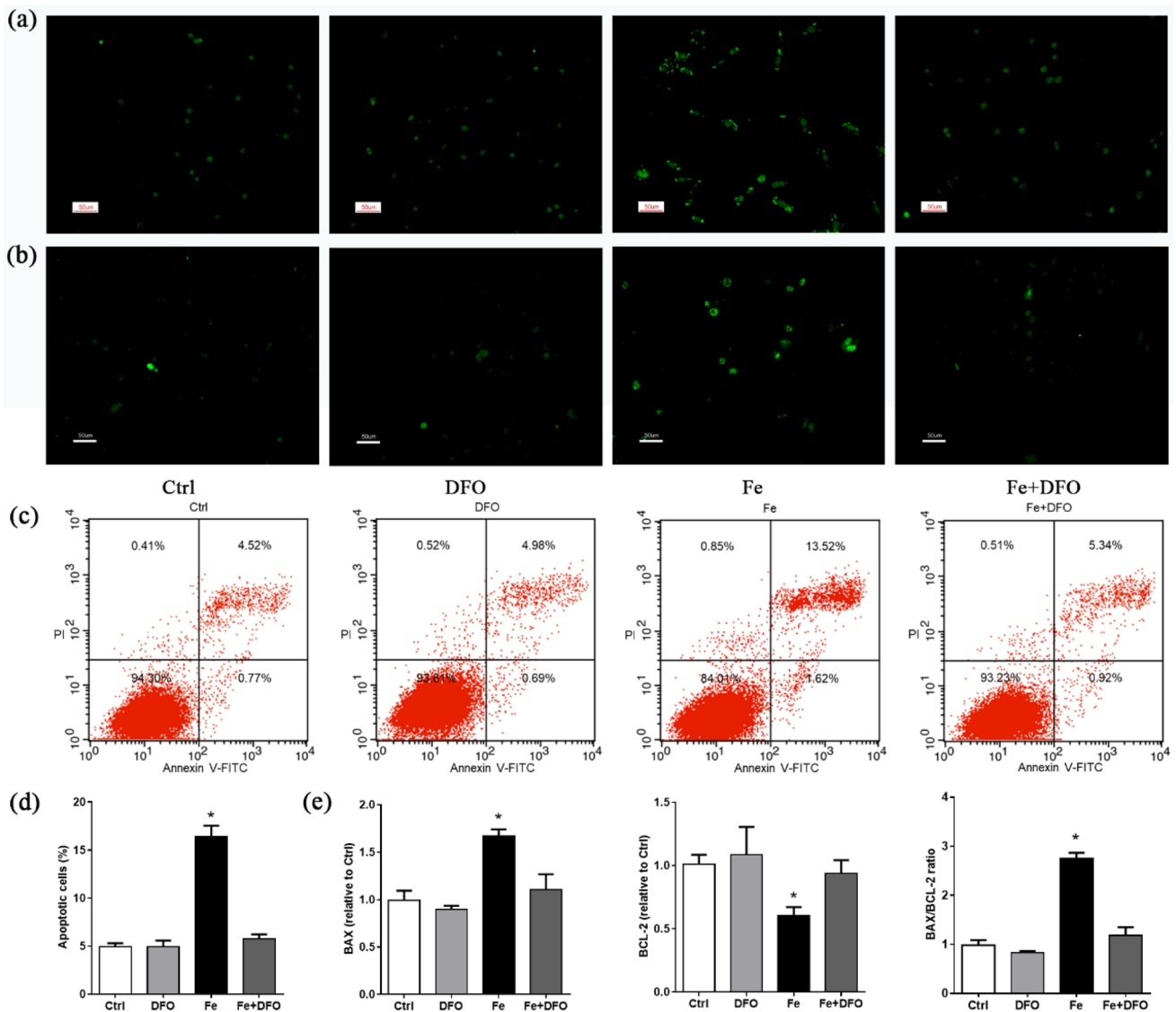
Fig. 2 Iron-induced apoptosis in osteocytes. TUNEL staining evaluated apoptosis in MLO-Y4 cells (**a**) and primary osteocytes (**b**); scale bar = 50 μm. **c** Flow cytometric analysis of osteocytes stained with Annexin V-FITC/PI to examined cell apoptosis. **d** Percentage of apoptosis rates were analyzed. **e** Gene expression of BAX, BCL-2, and BAX/BCL-2 ratio was determined by quantitative real-time PCR. Data are presented as the mean ± standard deviation ($n = 3$). *$P < 0.05$ compared with the Ctrl group

RANKL-blocking antibody abolished the osteocyte apoptosis-induced increase in osteoclast formation, bone resorption capacity, and actin rings formation (Fig. 6).

The CM from Apoptosis-Inhibited Osteocytes Prevents Osteoclastic Formation and Bone Resorption Capacity

To assess whether osteocyte apoptosis is necessary for increased osteoclast differentiation induced by the CM from iron-exposed osteocytes, we performed a pan-caspase inhibitor (QVD) to iron-exposed MLO-Y4 cells and primary osteocytes. TUNEL staining showed iron-induced osteocyte apoptosis was blocked by QVD in MLO-Y4 cells (Fig. 7a) and primary osteocytes (Fig. 7b). ELISA assay displayed QVD reduced the concentration of sRANKL in the CM from Fe-treated osteocytes (Fig. 7c). Furthermore, the osteocyte apoptosis-induced increase in osteoclast formation, bone resorption capacity, and actin rings formation in BMDMs was prevented by the CM derived from co-incubated MLO-Y4 cells (Fig. 7d, f, and h) and primary osteocytes (Fig. 7e, j, and i) with iron and QVD.
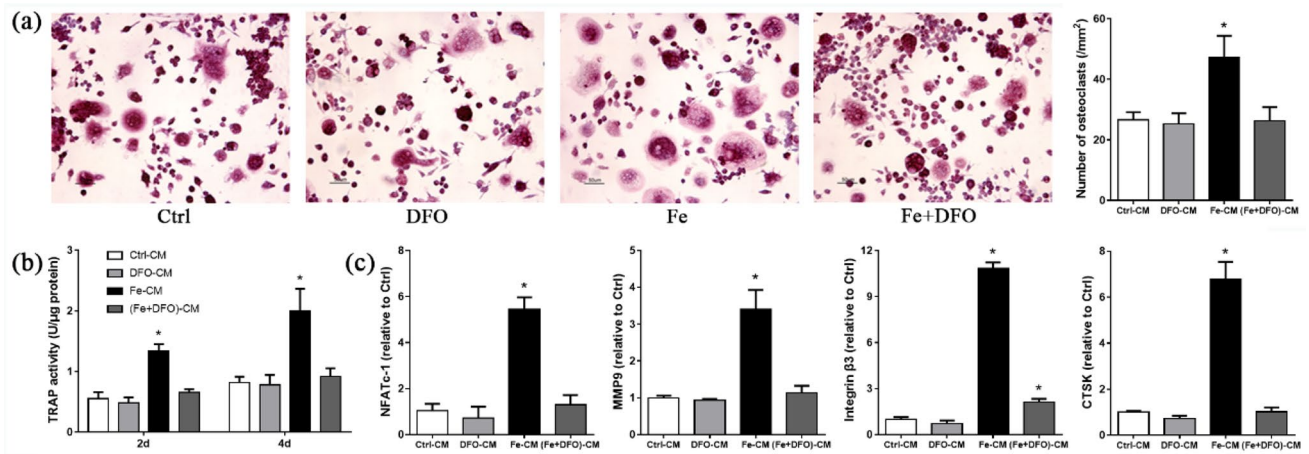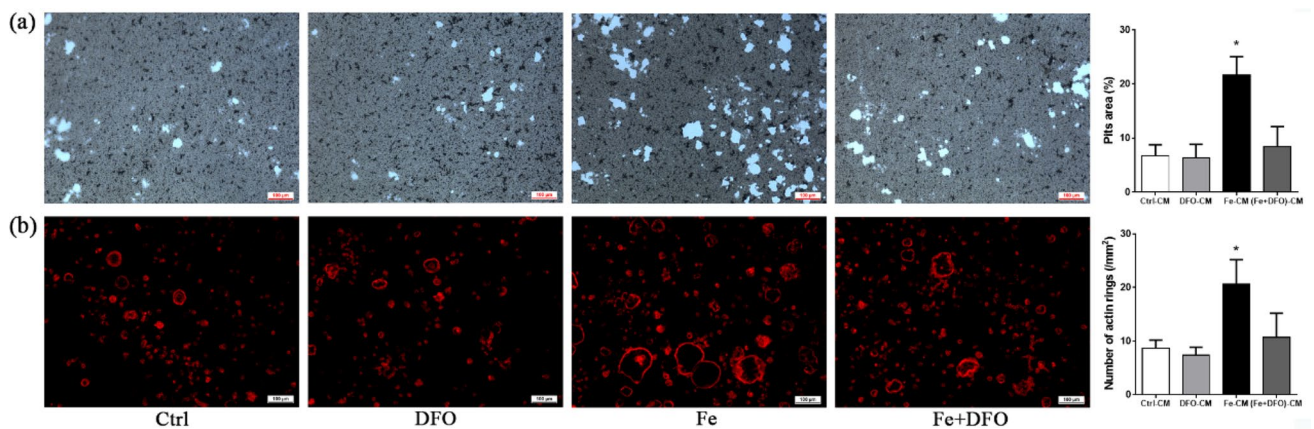
Fig. 3 CM from the iron-exposed osteocytes promoted osteoclast differentiation. **a** Osteoclast formation was evaluated by the TRAP staining; scale bar = 50 μm. **b** Osteoclastic TRAP activity was detected. **c** Representative gene expression related to osteoclast differentiation, including NFATc1, MMP9, Integrin β3, and CTSK was determined by quantitative real-time PCR. Data are presented as the mean ± standard deviation ($n = 3$). *$P < 0.05$ compared with the Ctrl group

Fig. 4 CM from the iron-exposed osteocytes promoted osteoclastic bone resorption capacity. **a** RAW264.7 cells were seeded in the Osteo Assay Surface 96-well plates to examined resorption pits to evaluated osteoclastic bone resorption capacity; scale bar = 100 μm. **b** Actin ring was stained by rhodamine-conjugated phalloidine staining; scale bar = 100 μm. Data are presented as the mean ± standard deviation ($n = 3$). *$P < 0.05$ compared with the Ctrl group

Discussion

Iron is involved in numerous cell biological activity, including DNA replication and cell respiration, thus it is essential for cell growth [19]. Iron-deprivation inhibits the proliferation of various mammalian cells [20]. DFO, an effective iron chelator, can inhibit osteoblastic proliferation and viability [7, 21]. In another aspect, excessive iron has a toxic effect on cells since iron is a highly transition metal and can catalyze the formation of damaging hydroxyl radicals. Numerous studies showed that the proliferation and viability of osteoblasts and bone marrow mesenchymal stem cells (BMMSCs) can be reduced by

iron overload [22–25]. Osteocyte, a terminally differentiated cells from osteoblasts and BMMSCs. Consistent with osteoblasts and BMMSCs, we also found low levels of iron induced by DFO and excessive iron from FAC significantly inhibited cell viability of osteocytes in a dose-dependent manner in the present study. These results indicate that iron in osteocytes requires be strictly regulated, and too high or too low levels of iron will damage osteocytes.

Iron overload exerts deleterious effects on various cell types and the mechanism of iron toxicity occurs are closely associated with apoptosis [26, 27]. In bone and bone marrow, previous studies also found cell apoptosis can be induced by iron overload in osteoblasts and BMMSCs [15, 16, 28, 29]. In this study, we demonstrated

Fig. 5 Effects of iron on gene expression and protein secretion of RANKL and OPG in osteocytes. **a** Gene expression of RANKL and OPG was examined by quantitative real-time PCR. **b** The secretion of soluble RANKL (sRANKL) and soluble OPG (sOPG) was determined by ELISA kit. Data are presented as the mean ± standard deviation ($n=3$). *$P<0.05$ compared with the Ctrl group
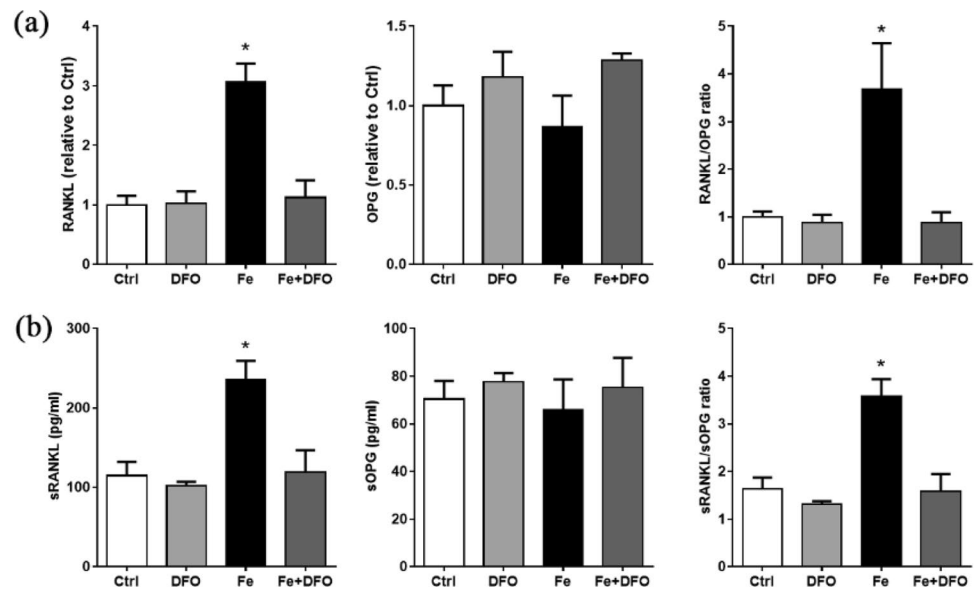

Fig. 6 Blocking RANKL abolished osteoclastic differentiation and bone resorption capacity induced by the CM from the iron-exposed osteocytes. **a** TRAP staining detected osteoclast formation; scale bar = 50 μm. **b** Pits formation assay evaluated bone resorption capacity; scale bar = 100 μm. **c** Actin ring was stained by rhodamine-conjugated phalloidine staining; scale bar = 100 μm. Data are presented as the mean ± standard deviation ($n=3$). *$P<0.05$
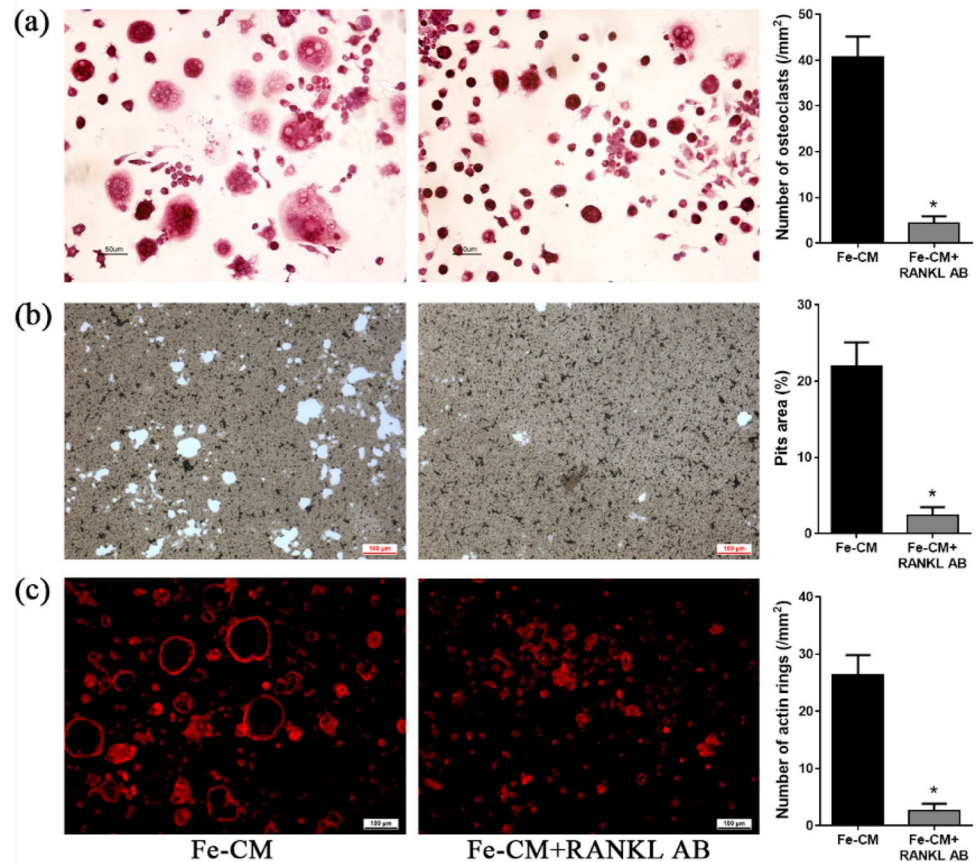
that iron overload markedly induced apoptosis in osteocytes. While the increased apoptosis of osteocytes can be rescued to the normal level by DFO. BAX as a proapoptotic factor and BCL-2 as an antiapoptotic factor have been implicated in the regulation of apoptosis of various cells [30]. Our PCR results showed that iron overload increased the gene expression of BAX and decreased BCL-2 expression in osteocytes, hence leads to a significant increase in the BAX/BCL-2 ratio was significantly increased under excessive iron stimulation. However, although excessive iron can induce osteocyte apoptosis in vitro, it is not clear whether iron overload can induce osteocyte apoptosis
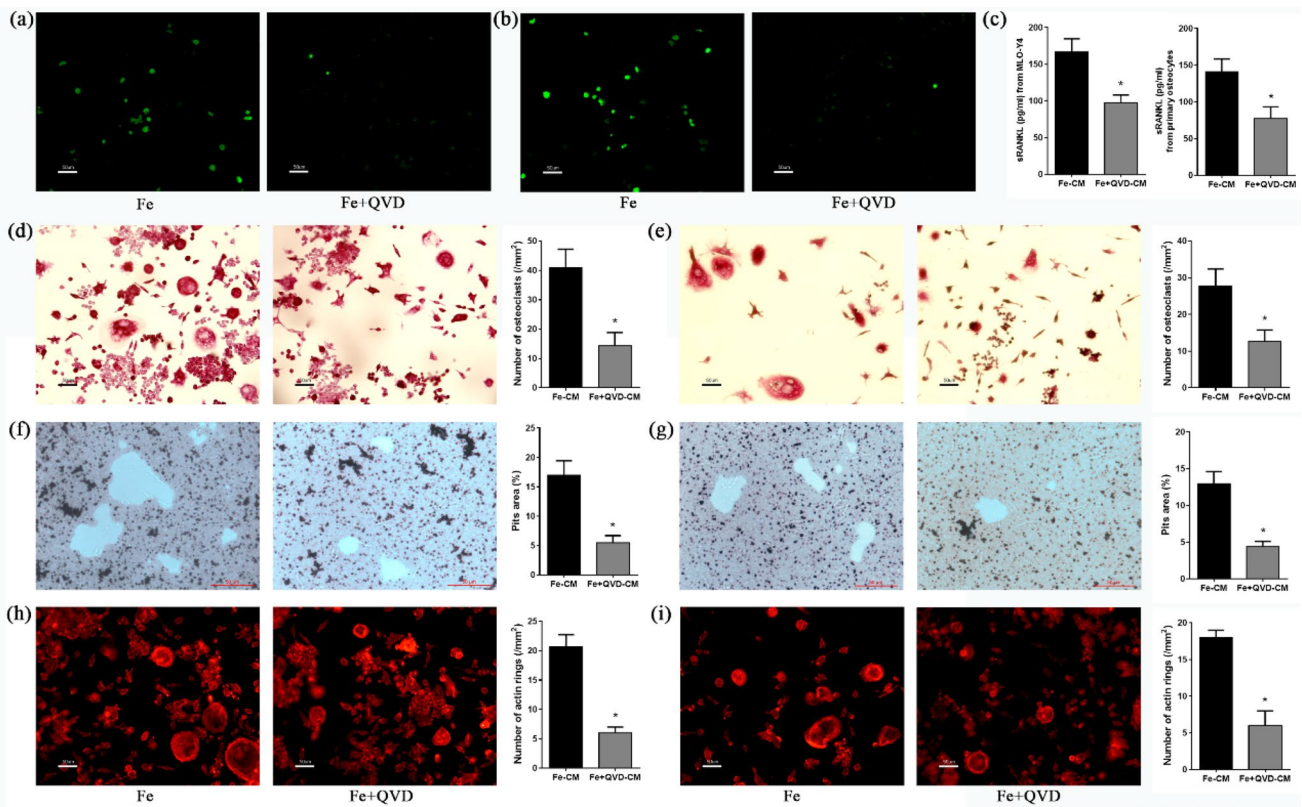
Fig. 7 CM from apoptosis-inhibited osteocytes prevented osteoclastic formation and bone resorption capacity in BMDMs. TUNEL staining evaluated apoptosis in MLO-Y4 cells (**a**) and primary osteocytes (**b**); scale bar = 50 μm. **c** The secretion of soluble RANKL (sRANKL) was determined by ELISA kit. TRAP staining detected osteoclast formation induced by the CM from MLO-Y4 cells (**d**) and primary osteocytes (**e**); scale bar = 50 μm. Pits formation assay evaluated bone resorption capacity triggered by the CM from MLO-Y4 cells (**f**) and primary osteocytes (**g**); scale bar = 50 μm. Actin ring formation induced by the CM from MLO-Y4 cells (**h**) and primary osteocytes (**i**) was stained by rhodamine conjugated phalloidine staining; scale bar = 50 μm. Data are presented as the mean ± standard deviation ($n = 3$). *$P < 0.05$

in vivo, and its exact mechanism needs to be explored by more experiments.

Osteoclasts, derived from the monocyte/macrophage haematopoietic lineage, play a crucial role in normal bone remodeling and calcium metabolism. Increased osteoclastic numbers and serum bone resorption makers have been found in bone surface of iron overload mice [2, 31]. Osteoclasts require high levels of iron to maintain high energy from mitochondrial metabolism to degrade bone matrix [32]. This seems to suggest that iron plays a direct role in promoting osteoclast differentiation and increases bone resorption in iron overloaded mice. Indeed, many in vitro studies have shown that excessive iron supplementation in culture medium can stimulate osteoclastic differentiation, activation, and bone resorption ability [4, 33, 34]. However, osteoclast activity can be effectively regulated by osteocyte through producing RANKL which is an essential pro-osteoclastogenic cytokine [35]. Present study demonstrated that the conditioned medium (CM) from excessive iron-treated osteocytes significantly enhanced osteoclastic differentiation,

bone resorption capacity, and actin rings formation. These data suggest that iron overload can indirectly promote osteoclast differentiation and function by regulating osteocytes. However, the use of osteo assay surface plates to evaluate the bone resorption capacity of osteoclasts is a limitation in this study. The osteo assay surface plate is only a mineral coated plate and do not contain any bone matrix. Therefore, it is possible that the resorptive effect would be different (i.e., bigger/smaller) if the cells were grown on bone or dentine. We will explore in more detail the effects of iron overload on bone resorption through osteocytes in future in vivo study.

RANKL is expressed in bone and bone marrow by variety of cell types, including osteoblasts, osteocytes, BMSCs and lymphocytes. It has been reported that osteocytes are the major secretory cells of RANKL and have a greater capacity to support osteoclastogenesis than osteoblasts and BMMSCs [9, 10]. OPG is an anti-osteoclastogenic factor, which can also be secreted by osteocytes. The binding of OPG to RANKL blocks its binding to receptor activator of NFκB (RANK) and further prevents the activation of

osteoclasts activity. Because OPG can be secreted in the same zone as RANKL, probably by the same type of cells that produce RANKL, the ratio of RANKL and OPG at a particular site is a main determinant of the magnitude of osteoclast formation and bone resorption at that location [36]. Studies also showed the increased RANKL expression in bone and elevated RANKL secretion in serum can be found in iron overloaded mice [2, 37]. However, the expression and secretion of OPG were not affected by iron overload, so the RANKL and OPG was also significantly enhanced by excessive iron in mice. Moreover, there is a great deal of evidence that osteocyte apoptosis triggers the production of RANKL in osteocytes [14, 38, 39]. Consistent with these data, our study showed iron overload induced the increase in osteocyte apoptosis and elevated the expression of RANKL, but had no effect on OPG expression in osteocytes. After apoptotic osteocytes were induced by excessive iron, and then incubated with serum-supplemented medium to obtain CM. ELISA assay found that the secretion of RANKL increased significantly, but the levels of OPG did not change obviously in the CM. The RANKL/OPG ratio was also significantly increased in excessive iron-exposed osteocytes and the CM.

In conclusion, we found that iron overload significantly promoted cell apoptosis in osteocyte-like MLO-Y4 cells and primary osteocytes derived from long bone of mice in the current study. We also found that the in vitro osteoclastogenesis and osteoclastic bone resorption capacity was significantly promoted by the CM from osteocytes with iron overload stimulation. The underlying mechanism by which the CM from iron-treated osteocytes enhanced osteoclast activity was that the secretion of sRANKL in the osteocytic CM was increased by excessive iron exposure. Moreover, addition of RANKL-blocking antibody completely abolished the apoptotic osteocyte-induced increase in osteoclast formation and bone resorption capacity. Our study represents the first effort identifying how osteocytes respond to iron overload and how osteocytes regulate the activity of osteoclasts under excessive iron exposure. This study is not only helpful to enrich our basic knowledge of the biological behaviors of osteocytes under iron overload, but also contributes to a more comprehensive understanding of the regulatory mechanism of iron overload on bone tissue and related bone diseases (e.g., osteoporosis).

Author Contributions All authors contributed to the study conception and design. Material preparation, data collection and analysis were performed by JY, DD, XL, and JZ. The first draft of the manuscript was written by JY and all authors commented on previous versions of the manuscript. All authors read and approved the final manuscript.

Compliance with Ethical Standards

Conflict of interest Jiancheng Yang, Dandan Dong, Xinle Luo, Jianhua Zhou, Peng Shang, and Hao Zhang declare that they have no conflict of interest.

Human and Animal Rights and Informed Consent Animal operation was conducted in accordance with the ethical guidelines for animals of the Medical and Experimental Animal Ethics Committee of Northwestern Polytechnic University.

References

1. Jeney V (2017) Clinical Impact and cellular mechanisms of iron overload-associated bone loss. Front Pharmacol 8:77. https://doi.org/10.3389/fphar.2017.00077
2. Tsay J, Yang Z, Ross FP, Cunningham-Rundles S, Lin H, Coleman R, Mayer-Kuckuk P et al (2010) Bone loss caused by iron overload in a murine model: importance of oxidative stress. Blood 116:2582–2589. https://doi.org/10.1182/blood-2009-12-260083
3. Yang Q, Jian J, Abramson SB, Huang X (2011) Inhibitory effects of iron on bone morphogenetic protein 2-induced osteoblastogenesis. J Bone Miner Res 26:1188–1196. https://doi.org/10.1002/jbmr.337
4. Ishii KA, Fumoto T, Iwai K, Takeshita S, Ito M, Shimohata N, Aburatani H et al (2009) Coordination of PGC-1beta and iron uptake in mitochondrial biogenesis and osteoclast activation. Nat Med 15:259–266. https://doi.org/10.1038/nm.1910
5. Wang L, Fang B, Fujiwara T, Krager K, Gorantla A, Li C, Feng JQ et al (2018) Deletion of ferroportin in murine myeloid cells increases iron accumulation and stimulates osteoclastogenesis in vitro and in vivo. J Biol Chem 293:9248–9264. https://doi.org/10.1074/jbc.RA117.000834
6. Kang H, Yan Y, Jia P, Yang K, Guo C, Chen H, Qi J et al (2016) Desferrioxamine reduces ultrahigh-molecular-weight polyethylene-induced osteolysis by restraining inflammatory osteoclastogenesis via heme oxygenase-1. Cell Death Dis 7:e2435. https://doi.org/10.1038/cddis.2016.339
7. Baschant U, Rauner M, Bulycheva E, Weidner H, Roetto A, Platzbecker U, Hofbauer LC (2016) Wnt5a is a key target for the pro-osteogenic effects of iron chelation on osteoblast progenitors. Haematologica 101:1499–1507. https://doi.org/10.3324/haematol.2016.144808
8. Robling AG, Bonewald LF (2020) The osteocyte: new insights. Annu Rev Physiol 82:485–506. https://doi.org/10.1146/annurev-physiol-021119-034332
9. Xiong J, Onal M, Jilka RL, Weinstein RS, Manolagas SC, O'Brien CA (2011) Matrix-embedded cells control osteoclast formation. Nat Med 17:1235–1241. https://doi.org/10.1038/nm.2448
10. Nakashima T, Hayashi M, Fukunaga T, Kurata K, Oh-Hora M, Feng JQ, Bonewald LF et al (2011) Evidence for osteocyte regulation of bone homeostasis through RANKL expression. Nat Med 17:1231–1234. https://doi.org/10.1038/nm.2452
11. Aguirre JI, Plotkin LI, Stewart SA, Weinstein RS, Parfitt AM, Manolagas SC, Bellido T (2006) Osteocyte apoptosis is induced by weightlessness in mice and precedes osteoclast recruitment and

bone loss. J Bone Miner Res 21:605–615. https://doi.org/10.1359/jbmr.060107

12. Kennedy OD, Herman BC, Laudier DM, Majeska RJ, Sun HB, Schaffler MB (2012) Activation of resorption in fatigue-loaded bone involves both apoptosis and active pro-osteoclastogenic signaling by distinct osteocyte populations. Bone 50:1115–1122. https://doi.org/10.1016/j.bone.2012.01.025

13. Kennedy OD, Laudier DM, Majeska RJ, Hui B, Sun HB, Schaffler MB (2014) Osteocyte apoptosis is required for production of osteoclastogenic signals following bone fatigue in vivo. Bone 64:132–137. https://doi.org/10.1016/j.bone.2014.03.049

14. Cabahug-Zuckerman P, Frikha-Benayed D, Majeska RJ, Tuthill A, Yakar S, Judex S, Schaffler MB (2016) Osteocyte apoptosis caused by hindlimb unloading is required to trigger osteocyte RANKL production and subsequent resorption of cortical and trabecular bone in mice femurs. J Bone Miner Res 31:1356–1365. https://doi.org/10.1002/jbmr.2807

15. Yuan Y, Xu F, Cao Y, Xu L, Yu C, Yang F, Zhang P et al (2018) Iron accumulation leads to bone loss by inducing mesenchymal stem cell apoptosis through the activation of Caspase3. Biol Trace Elem Res. https://doi.org/10.1007/s12011-018-1388-9

16. Tian Q, Wu S, Dai Z, Yang J, Zheng J, Zheng Q, Liu Y (2016) Iron overload induced death of osteoblasts in vitro: involvement of the mitochondrial apoptotic pathway. PeerJ 4:e2611. https://doi.org/10.7717/peerj.2611

17. Stern AR, Stern MM, Van Dyke ME, Jahn K, Prideaux M, Bonewald LF (2012) Isolation and culture of primary osteocytes from the long bones of skeletally mature and aged mice. Biotechniques 52:361–373. https://doi.org/10.2144/0000113876

18. Wang P, Tang C, Wu J, Yang Y, Yan Z, Liu X, Shao X et al (2019) Pulsed electromagnetic fields regulate osteocyte apoptosis, RANKL/OPG expression, and its control of osteoclastogenesis depending on the presence of primary cilia. J Cell Physiol 234:10588–10601. https://doi.org/10.1002/jcp.27734

19. van Swelm RPL, Wetzels JFM, Swinkels DW (2019) The multifaceted role of iron in renal health and disease. Nat Rev Nephrol. https://doi.org/10.1038/s41581-019-0197-5

20. Nurtjahja-Tjendraputra E, Fu D, Phang JM, Richardson DR (2006) Iron chelation regulates cyclin D1 expression via the proteasome: a link to iron deficiency-mediated growth suppression. Blood 109:4045–4054. https://doi.org/10.1182/blood-2006-10-047753

21. Zhao GY, Zhao LP, He YF, Li GF, Gao C, Li K, Xu YJ (2012) A comparison of the biological activities of human osteoblast hFOB1.19 between iron excess and iron deficiency. Biol Trace Elem Res 150:487–495. https://doi.org/10.1007/s12011-012-9511-9

22. Yang F, Yang L, Li Y, Yan G, Feng C, Liu T, Gong R et al (2017) Melatonin protects bone marrow mesenchymal stem cells against iron overload-induced osteogenic differentiation dysfunction and senescence. J Pineal Res. https://doi.org/10.1111/jpi.12422

23. Lertsuwan K, Nammultriputtar K, Nanthawuttiphan S, Phoaubon S, Lertsuwan J, Thongbunchoo J, Wongdee K et al (2018) Ferrous and ferric differentially deteriorate proliferation and differentiation of osteoblast-like UMR-106 cells. Biometals 31:873–889. https://doi.org/10.1007/s10534-018-0130-6

24. Cen WJ, Feng Y, Li SS, Huang LW, Zhang T, Zhang W, Kong WD et al (2018) Iron overload induces G1 phase arrest and autophagy in murine preosteoblast cells. J Cell Physiol 233:6779–6789. https://doi.org/10.1002/jcp.26405

25. Yao X, Jing X, Guo J, Sun K, Deng Y, Zhang Y, Guo F et al (2019) Icariin protects bone marrow mesenchymal stem cells against iron overload induced dysfunction through mitochondrial fusion and fission, PI3K/AKT/mTOR and MAPK Pathways. Front Pharmacol 10:163. https://doi.org/10.3389/fphar.2019.00163

26. Yang M, Chan S, Ye J, ChiFung CG (2013) TPO exerts a protective effect on iron-overload induces apoptosis in cardiomyocytes via mitochondrial pathways. Blood 122:4668–4668. https://doi.org/10.1182/blood.V122.21.4668.4668

27. Wang GS, Eriksson LC, Xia L, Olsson J, Stal P (1999) Dietary iron overload inhibits carbon tetrachloride-induced promotion in chemical hepatocarcinogenesis: effects on cell proliferation, apoptosis, and antioxidation. J Hepatol 30:689–698. https://doi.org/10.1016/s0168-8278(99)80201-3

28. Yang F, Li Y, Yan G, Liu T, Feng C, Gong R, Yuan Y et al (2017) Inhibition of iron overload-induced apoptosis and necrosis of bone marrow mesenchymal stem cells by melatonin. Oncotarget. https://doi.org/10.18632/oncotarget.16382

29. Ke JY, Cen WJ, Zhou XZ, Li YR, Kong WD, Jiang JW (2017) Iron overload induces apoptosis of murine preosteoblast cells via ROS and inhibition of AKT pathway. Oral Dis 23:784–794. https://doi.org/10.1111/odi.12662

30. Kundson CM, SJ, Korsmeyer (1997) Bcl-2 and Bax function independently to regulate cell death. Nat Genet 16:358–363. https://doi.org/10.1038/ng0897-358

31. Xiao W, Bin C, Jingyue S, Yu J, Hui Z, Peng Z, Beibei F et al (2018) Iron-induced oxidative stress stimulates osteoclast differentiation via NF-kappaB signaling pathway in mouse model. Metabolism. https://doi.org/10.1016/j.metabol.2018.01.005

32. Roodman GD (2009) Osteoclasts pump iron. Cell Metab 9:405–406. https://doi.org/10.1016/j.cmet.2009.04.005

33. Xie W, Lorenz S, Dolder S, Hofstetter W (2016) Extracellular Iron is a modulator of the differentiation of osteoclast lineage cells. Calcif Tissue Int 98:275–283. https://doi.org/10.1007/s00223-015-0087-1

34. Zhang J, Hu W, Ding C, Yao G, Zhao H, Wu S (2019) Deferoxamine inhibits iron-uptake stimulated osteoclast differentiation by suppressing electron transport chain and MAPKs signaling. Toxicol Lett 313:50–59. https://doi.org/10.1016/j.toxlet.2019.06.007

35. Zhao S, Kato Y, Zhang Y, Harris S, Ahuja S, Bonewald L (2002) MLO-Y4 osteocyte-like cells support osteoclast formation and activation. J Bone Miner Res 17:2068–2079. https://doi.org/10.1359/jbmr.2002.17.11.2068

36. O'Brien CA, Nakashima T, Takayanagi H (2013) Osteocyte control of osteoclastogenesis. Bone 54:258–263. https://doi.org/10.1016/j.bone.2012.08.121

37. Jia P, Xu YJ, Zhang ZL, Li K, Li B, Zhang W, Yang H (2012) Ferric ion could facilitate osteoclast differentiation and bone resorption through the production of reactive oxygen species. J Orthop Res 30:1843–1852. https://doi.org/10.1002/jor.22133

38. McCutcheon S, Majeska RJ, Spray DC, Schaffler MB, Vazquez M (2020) Apoptotic osteocytes induce RANKL production in bystanders via purinergic signaling and activation of pannexin channels. J Bone Miner Res. https://doi.org/10.1002/jbmr.3954

39. Plotkin LI, Gortazar AR, Davis HM, Condon KW, Gabilondo H, Maycas M, Allen MR et al (2015) Inhibition of osteocyte apoptosis prevents the increase in osteocytic receptor activator of nuclear factor kappaB ligand (RANKL) but does not stop bone resorption or the loss of bone induced by unloading. J Biol Chem 290:18934–18942. https://doi.org/10.1074/jbc.M115.642090